



IONMIX - A Code for Computing the Equation of State and Radiative Properties of LTE and Non-LTE Plasmas

J.J. MacFarlane

December 1987

UWFDM-750

Comp. Phys. Commun. 56 (1989) 259.

***FUSION TECHNOLOGY INSTITUTE
UNIVERSITY OF WISCONSIN
MADISON WISCONSIN***

DISCLAIMER

This report was prepared as an account of work sponsored by an agency of the United States Government. Neither the United States Government, nor any agency thereof, nor any of their employees, makes any warranty, express or implied, or assumes any legal liability or responsibility for the accuracy, completeness, or usefulness of any information, apparatus, product, or process disclosed, or represents that its use would not infringe privately owned rights. Reference herein to any specific commercial product, process, or service by trade name, trademark, manufacturer, or otherwise, does not necessarily constitute or imply its endorsement, recommendation, or favoring by the United States Government or any agency thereof. The views and opinions of authors expressed herein do not necessarily state or reflect those of the United States Government or any agency thereof.

**IONMIX - A Code for Computing the
Equation of State and Radiative Properties of
LTE and Non-LTE Plasmas**

J.J. MacFarlane

Fusion Technology Institute
University of Wisconsin
1500 Engineering Drive
Madison, WI 53706

<http://fti.neep.wisc.edu>

December 1987

UWFDM-750

IONMIX - A Code for Computing the Equation of State
and Radiative Properties of LTE and Non-LTE Plasmas

J.J. MacFarlane

Fusion Technology Institute
1500 Johnson Drive
University of Wisconsin-Madison
Madison, Wisconsin 53706

December 1987

UWFD-750

To be submitted to Computer Physics Communications for publication.

**IONMIX - A Code for Computing the Equation of State
and Radiative Properties of LTE and Non-LTE Plasmas**

Joseph J. MacFarlane

Fusion Technology Institute, University of Wisconsin-Madison,
1500 Johnson Drive, Madison, WI 53706 USA

Program Summary

Title of program: IONMIX

Catalogue number:

Program obtainable from: CPC Program Library, Queen's University of Belfast,
Northern Ireland.

Computer: VAX 8600; Installation: Madison Academic Computing Center,
University of Wisconsin, Madison, Wisconsin, USA

Operating system: VAX/VMS

Programming language: FORTRAN 77

High speed storage required: 156,000 words

No. of bits in a word: 32

Overlay structure: none

Peripherals used: line printer, ten disk files

No. of lines in combined program and test deck: 5,043

CPC Library subprograms used: none

Keywords: LTE and non-LTE plasma physics, equations of state,
opacities, semi-classical atomic physics.

Nature of the physical problem

The thermodynamic and radiative properties of hot plasmas are often required in studying a wide variety of physical phenomena. Examples of these include hydrodynamic and radiative energy transport in astrophysical and fusion plasmas [1,2]. The physical conditions of plasmas considered in this paper range from a relatively high density regime, where three-body collisions

dominate all atomic processes, to a low density regime where two-body radiative processes become important. In the collisionally dominated regime, the plasma is said to be in local thermodynamic equilibrium (LTE). Occasionally, problems arise in which portions of a fluid can migrate back and forth through the LTE and non-LTE regimes. One example of this is the evolution of the background gas as it responds to an inertial confinement fusion (ICF) pellet explosion. In such problems, the effects of both two-body and three-body atomic processes must be considered simultaneously when calculating the ionization and excitation populations, as well as the plasma's radiative properties. The IONMIX code does precisely this in computing the equation of state and multigroup opacities needed to describe the absorption, emission, and transport of radiation for both LTE and non-LTE plasmas.

Method of solution

The steady-state ionization and excitation populations are calculated using detailed balance arguments. The atomic processes considered are: collisional ionization and recombination, radiative recombination, dielectronic recombination, collisional excitation and deexcitation, and radiative decay. At relatively low densities, two-body recombination is balanced by collisional ionization. At higher densities, three-body collisional recombination is dominant, in which case the LTE populations are computed using the Saha equation [3]. Ground state ionization energies are taken from the calculations of Carlson et al. [4], and the excitation energy levels are approximated using a modified Bohr model. After the populations are computed, the specific energy, average charge state, and pressure are readily evaluated. Thermal derivatives, such as the heat capacity, are computed numerically.

Contributions from bremsstrahlung, photoionization, bound-bound transitions (lines), Thomson scattering, and plasma waves are included in

calculating the absorption, emission, and scattering coefficients. The coefficients are calculated at a large number (~ several hundred) of well-placed photon energies, and numerically integrated to determine the Planck and Rosseland group opacities, mean opacities, and plasma cooling rates.

Restrictions on the complexity of the problem

The IONMIX code assumes that contributions to the internal energy arising from interparticle potentials is small compared to the thermal energy. This dictates that the ion densities be $\lesssim 10^{20} (T/\langle Z \rangle)^3 \text{ cm}^{-3}$, where T is the temperature in eV, and $\langle Z \rangle$ is the mean charge state. In addition, temperatures must be high enough ($\gtrsim 10^4 \text{ K}$) that molecular effects, such as vibrational and rotational contributions, can be ignored. Also, the radiation energy density is assumed to be small so that ionization and excitation occur collisionally.

Maximum values for the number of gases (10), atomic number of each gas species (54), opacity groups (50), temperatures (20), and densities (20) are constrained by array sizes. However, with rather simple modifications to the code, these limits can be changed.

Typical running time

The CPU time required to compute all thermodynamic and radiative properties is about 0.2 seconds/(gas species)/(atomic number) element at each temperature, density point.

Unusual features of the program

The IONMIX code is written in FORTRAN 77 with the sole exception that namelist input is used. Two VAX system subroutines are called to provide the time and date of the calculation. Otherwise, the code is transportable to other mainframe computers.

References

- [1] M. Uesaka, R.R. Peterson, G.A. Moses, Nucl. Fusion 24 (1984) 1137; R.V. Jensen, D.E. Post, W.H. Grasberger, C.B. Tarter, and W.A. Lokke, Nucl. Fusion 17 (1977) 1187.
- [2] See, e.g., "Radiation Hydrodynamics in Stars and Compact Objects," edited by D. Mihalas and K.-H.A. Winkler (Springer-Verlag, New York, 1986).
- [3] D. Mihalas, "Stellar Atmospheres" (W.H. Freeman, San Francisco, 1978).
- [4] T.A. Carlson, C.W. Nestor, Jr., N. Wasserman, and J.D. McDowell, At. Data Nucl. Data Tables 2 (1970) 63.

1. INTRODUCTION

The equation of state and radiative properties of plasmas are often required to study the physical properties of laboratory and astrophysical plasmas [1,2]. Quite often the conditions in a problem are such that the plasma can be considered to be at either of two extremes: (1) local thermodynamic equilibrium (LTE), in which case 3-body collisions dominate all atomic processes, or (2) non-LTE, "coronal" equilibrium, where the gas density is sufficiently low that 2-body radiative effects are the dominant mechanism of recombination and deexcitation. However, a number of problems exist in which the plasma can migrate between these two extremes, thus requiring a solution in which both 2-body and 3-body atomic processes are fully considered. Examples of this include stellar atmospheres, and inertial confinement fusion (ICF) target chambers, where gas densities can vary from $\sim 10^{14}$ to 10^{18} ions/cm³ and temperatures from $\sim 10^4$ to 10^7 K.

Below, we describe the features of IONMIX, a computer code which calculates the equation of state and radiative properties of both LTE and non-LTE

plasmas. IONMIX does this by fully considering both radiative and collisional atomic processes when computing the ionization and excitation populations, and their subsequent effects on the plasma radiative properties. The results are applicable to plasmas where: (1) gas densities are low enough that inter-particle potentials can be ignored, (2) the radiation energy field can be neglected in computing the ionization and excitation rates (i.e., collisions dominate these processes), and (3) molecular effects are unimportant.

The IONMIX code computes the steady-state ionization and excitation populations for a mixture of up to 10 different atomic species. The radiative absorption, emission, and scattering coefficients are calculated at a large number (~ several hundred) of photon energies, and integrated over selected energy intervals to determine the multigroup Planck and Rosseland mean opacities. The code also calculates the thermodynamic properties of the plasma, such as the specific energy, average charge state, pressure, and heat capacity.

2. ATOMIC PROCESSES

2.1. Ionization Populations

The ionization populations for IONMIX are computed for steady-state conditions using detailed balance arguments. The atomic processes considered are collisional ionization, radiative recombination, dielectronic recombination, and collisional recombination. The hydrogenic ion approximation is used in computing the various reaction rates.

Throughout this paper, the subscripts j and k refer to the ionization state and gas species, respectively. The units generally used in this paper and throughout the code are as follows:

energy	eV	ion density	cm ⁻³
temperature	eV	electron density	cm ⁻³
time	s	mass density	g/cm ³
charge	esu	specific energy	J/g
length	cm	heat capacity	J/g/eV

Under steady-state conditions, the number of ions in the j^{th} ionization state species is given by

$$N_{jk} = N_k \frac{\prod_{m=0}^{j-1} R_{m,m+1}}{1 + \sum_{l=1}^{Z_k} \prod_{m=0}^{l-1} R_{m,m+1}}, \quad (2-1)$$

where $N_k = \sum_{j=0}^{Z_k} N_{jk}$ is the total number of species k nuclei and Z_k is the atomic number of species k . $R_{m,m+1}$ is the ratio of the collisional ionization rate, C_{coll} , to the sum of the recombination rates between states m and $m+1$:

$$R_{m,m+1} = C_{\text{coll}}^m / (\alpha_{\text{rr}}^{m+1} + \alpha_{\text{dr}}^{m+1} + \alpha_{\text{coll}}^{m+1}). \quad (2-2)$$

α_{rr} , α_{dr} , and α_{coll} are the radiative, dielectronic, and collisional recombination rates, respectively. Collisional recombination is a 3-body process involving two electrons and an ion. Radiative and dielectronic recombination are 2-body processes in which the excess energy is carried away by a photon as opposed to a second electron. Because of its greater dependence on the electron density, collisional effects dominate the recombination process in the high density limit.

Collisional ionization involves the reaction $X^{j+} + e^- \rightarrow X^{(j+1)+} + e^- + e^-$, where X^{j+} represents the j^{th} ionization stage of atom X . The rate at

which this reaction takes place is [3]

$$C_{\text{coll}}^j = (1.09 \times 10^{-6} \text{ cm}^{-3} \text{ s}^{-1}) n_e n_j T^{1/2} \cdot e^{-x_j} (1 - e^{-x_j}) \phi_j^{-2} r_j, \quad (2-3)$$

where n_e and n_j are the densities of electrons and ions in the j^{th} ionization state, respectively. The subscript k is assumed. T is the electron temperature in eV, ϕ_j is the ionization potential in eV, and $x_j \equiv \phi_j/T$. We use the empirical formula given in reference [3] for the Gaunt factor, r_j .

IONMIX uses the calculated ionization potentials of Carlson et al. [4] as default values for several elements. These elements are: H, He, Li, Be, C, N, O, Ne, Mg, Si, S, Ar, Fe, Kr, and Xe. The ionization potentials for other elements must be supplied by the user through an input file. The user also has the option of overriding the default values for the ionization potentials (see sections 5 and 8).

The collisional recombination rate, which is the reverse process of collisional ionization, can be written as

$$\alpha_{\text{coll}}^{j+1} = C_{\text{coll}}^j (1.66 \times 10^{-22}) n_e T^{-3/2} e^{x_j} (U_{j+1}/U_j) \quad (2-4)$$

where C_{coll}^j is defined in eq. (2-3), and U_j and U_{j+1} are the electronic partition functions for the j^{th} and $(j+1)^{\text{st}}$ ionization stages. In the limit of high densities, radiative processes are small, and eqs. (2-1) through (2-4) simply produce the well-known Saha equation [5].

For the radiative recombination rate, we assume a Gaunt factor of unity and use the expression derived by Seaton [6]:

$$\alpha_{\text{rr}}^{j+1} = (5.20 \times 10^{-14} \text{ cm}^{-3} \text{ s}^{-1}) n_e n_{j+1} (j+1) x_j^{3/2} e^{x_j} E_1(x_j). \quad (2-5)$$

Polynomial fits [7] are used to evaluate the first exponential integral, $E_1(x)$.

Dielectronic recombination becomes important at relatively high temperatures and low densities. For the dielectronic recombination rate, we use the modifications of Post et al. [3] to the formulae originally proposed by Burgess [8]:

$$\alpha_{dr}^{j+1} = (2.40 \times 10^{-9} \text{cm}^{-3} \text{s}^{-1}) n_e n_{j+1} T^{-3/2} \quad (2-6)$$

$$\cdot B(j+1) D(j+1) \sum_n f_{ni} A(y) e^{-\bar{E}_{ni}(j)/T}$$

where i is the initial electronic state of the ion, and the summation is over all bound states n . f_{ni} is the oscillator strength for the exciting transition (see section 2.2). The expressions for B and \bar{E} are

$$B(z \equiv j+1) = z^{1/2} (z+1)^{5/2} (z^2 + 13.4)^{-1/2}$$

$$E_{ni}(j) = 13.6 \text{ eV } (j+2)^2 (\nu_i^{-1} - \nu_n^{-1})/a$$

where

$$a = 1 + 0.015 (j+1)^3/(j+2)^2,$$

and ν_i and ν_n are the effective principal quantum numbers of state i and n , respectively. The formulae for $A(y)$ and $D(j+1)$ depend on whether a change in the principal quantum number occurs during the excitation. They are defined as

$$A(y) = \begin{cases} y^{1/2} / (1 + 0.105 y + 0.015 y^2), & \Delta n = 0 \\ y^{1/2} / (2 + 0.420 y + 0.060 y^2), & \Delta n \neq 0 \end{cases}$$

$$D(q \equiv j+2) = \begin{cases} N_t / (n_t + 200), & \Delta n = 0 \\ (q N_t)^2 / [(q N_t)^2 + 667], & \Delta n \neq 0 \end{cases}$$

where

$$N_t = [1.51 \times 10^{17} (j+1)^6 T^{1/2} / n_e]^{1/7}.$$

$D(q)$ represents a reduction factor to account for increased collisional effects at high densities. N_t is also used for the upper limit of the summation in eq. (2-6).

The ionization populations are found by solving eq. (2-1) using the rates described above. In practice, an iterative method is used because the electron density is not known in advance. At low densities, the $R_{m,m+1}$'s in eq. (2-2) are only weakly dependent on the electron density. This is due to the fact that the dielectronic recombination rate is slightly nonlinear in the electron density. At relatively high densities, 3-body collisional recombination dominates, and $R_{m,m+1}$ is inversely proportional to the electron density. A Newton-Raphson iteration scheme is used to determine the self-consistent electron density.

Figure 2-1 shows the computed ionization fractions for a low density carbon plasma as a function of the electron temperature. The results for the odd ionization states (C^{1+} , C^{3+} , and C^{5+}) are represented by the dashed curves, while the even ionization fractions are represented by the solid curves. At temperatures above ~ 200 eV, essentially all of the carbon becomes fully ionized. It can also be seen that C^{4+} is rather abundant over a relatively large temperature range (10 to 50 eV). This is a result of the rather large amount of energy required to ionize an electron from the 1s shell.

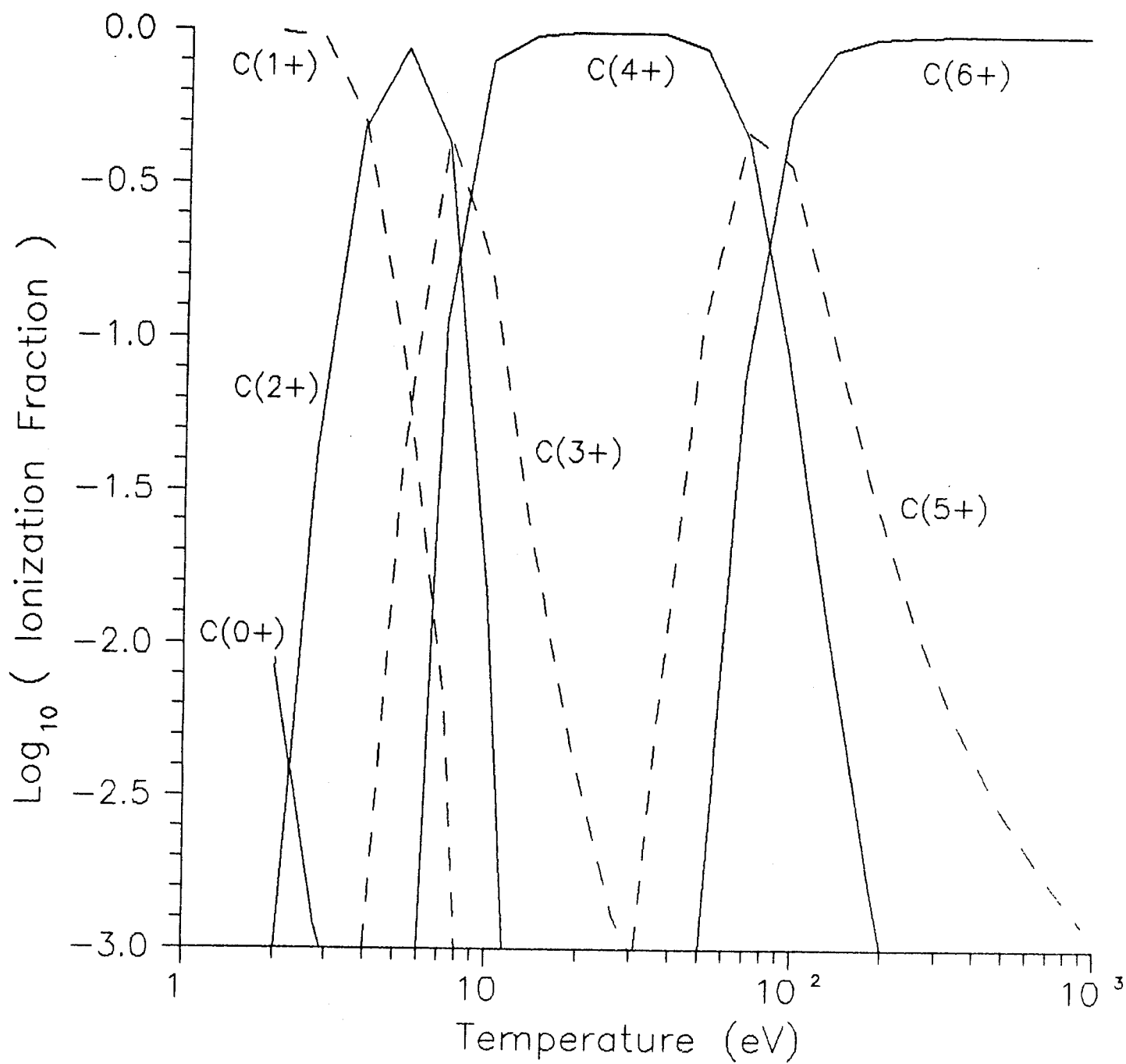


Figure 2-1. Fraction of carbon ions in each ionization state as a function of temperature. The dashed and solid curves represent the odd and even ionization states, respectively.

2.2. Excitation Populations

After the ionization populations are determined, IONMIX computes the excitation populations for each ion. Here, the populations of each excited state are calculated by balancing the collisional excitation rate with the sum of the collisional deexcitation and radiative decay rates. Again, in the high density limit collisional processes dominate, and the populations are computed using Boltzmann's statistics [9]. In the low density limit, the radiative decay rate will exceed the collisional deexcitation rate.

The collisional excitation rate for the electronic transition $m \rightarrow n$ is given by [10]

$$C_{\text{exc}}^{nm} = (1.58 \times 10^{-5} \text{cm}^{-3} \text{s}^{-1}) n_e n_n g_{nm} f_{nm} \frac{e^{-\Delta E_{nm}/T}}{(\Delta E_{nm} T^{1/2})} \quad (2-7)$$

where n_n is the density of ions in the n^{th} excitation state (the j and k indices have been dropped for convenience). f_{nm} and g_{nm} are the oscillator strength and Gaunt factor for the transition, and ΔE_{nm} is the energy of the transition in eV.

For transitions in which the principal quantum number does not change, we use a Bohr-like model to estimate the transition energies. The energy relative to the continuum of an ion with the outermost electron residing in shell n is given by

$$E_{n,j} = -\phi_j (n_0/n)^2, \quad n \geq n_0, \quad (2-8)$$

where n_0 represents the principal quantum number of the outermost electron in its ground state, and ϕ_j is the ionization potential. Thus, the change in energy as the electron is excited from state n to m is

$$\Delta E_{nm} = \Phi_j n_0^2 \left(\frac{1}{n^2} - \frac{1}{m^2} \right), \quad m > n. \quad (2-9)$$

The oscillator strengths for $\Delta n \neq 0$ transitions are computed using the hydrogenic approximation [11], while the Gaunt factors are based on the work of Van Regemorter [10]. For $\Delta n=0$ transitions, we use the oscillator strengths and Gaunt factors tabulated by reference [3].

The collisional deexcitation rate for the $m \rightarrow n$ transition is determined from the principle of detailed balance and Boltzmann statistics:

$$\alpha_{cdx}^{nm} = C_{exc}^{nm} \cdot \frac{g_m}{g_n} e^{-\Delta E_{nm}/T} \quad (2-10)$$

where g_n and g_m are the statistical weights of states n and m , respectively. The radiative decay rate is calculated from the Einstein coefficient for spontaneous emission:

$$\alpha_{rd}^{nm} = (4.32 \times 10^7 \text{ cm}^{-3} \text{ s}^{-1}) n_m (\Delta E_{nm})^2 f_{nm} \frac{g_n}{g_m}. \quad (2-11)$$

The relative excitation populations are then found by equating the forward and reverse rates in eqs. (2-9) through (2-11). This gives

$$\frac{n_m}{n_n} = \frac{(g_m/g_n) e^{-\Delta E_{nm}/T}}{1 + [3.65 \times 10^{-13} (\Delta E_{nm})^3 T^{1/2} / (n_e g_{nm})]}. \quad (2-12)$$

The above expression shows that the radiative decay term (i.e., the second term in the denominator) becomes less important as the electron density increases. The actual populations are obtained by normalizing the relative fractions in eq. (2-12) to the total number of ions in each ionization stage.

3. EQUATIONS OF STATE

After the ionization and excitation populations are determined, calculation of the equation of state properties is straightforward. The internal energies are computed relative to the ground state energy of the neutral atom of each species. Thus, the specific energy for an arbitrary mixture of ions is

$$E = \frac{n_{\text{tot}}}{\rho} \left\{ \frac{3}{2} (1 + \langle Z \rangle) T + \sum_k f_k \sum_{j=1}^{Z_k} f_{jk} \left[\left(\sum_{l=0}^{j-1} \phi_{lk} \right) + \left(\sum_{i=n_0+1} f_{ijk} (\Delta E_{in_0})_{jk} \right) \right] \right\} \quad (3-1)$$

where ρ is the mass density and n_{tot} is the total number density of nuclei. The relative species, ionization, and excitation fractions are defined by

$$f_k = \frac{n_k}{n_{\text{tot}}}, \quad f_{jk} = \frac{n_{jk}}{n_k}, \quad \text{and} \quad f_{ijk} = \frac{n_{ijk}}{n_{jk}}$$

where n_k , n_{jk} , and n_{ijk} refer to the number density of nuclei of gas species k , the j^{th} ionization state of species k , and the i^{th} excitation state of the j^{th} ionization state of species k , respectively. The ϕ_{lk} are the ionization potentials, and ΔE_{in_0} the excitation energies with respect to the ground state energy of each ion. The last two terms on the right-hand side of eq. (3-1) represent the energy stored in ionization and excitation, respectively. The average charge state is

$$\langle Z \rangle = \sum_k f_k \sum_{j=1}^{Z_k} f_{jk} \cdot j. \quad (3-2)$$

Figure 3-1 shows the average charge state for Ne as a function of ion density at 3 different temperatures. The usual IONMIX results (solid curves) are compared with those computed using only 3-body recombination (Saha ionization model) and only 2-body recombination (coronal ionization model). This figure shows that a neon plasma with a density $\sim 10^{18} - 10^{22} \text{ cm}^{-3}$ will move from the LTE to non-LTE regime when isochorically heated from $\sim 1 \text{ eV}$ to $\sim 10^2 \text{ eV}$.

Finally, since the interparticle potential energies are assumed to be small, the pressure is simply a function of the number of free particles and the temperature:

$$P = (1 + \langle Z \rangle) n_{\text{tot}} k T, \quad (3-3)$$

where T represents the temperature of both the electrons and ions (assumed to be in equilibrium). In addition, IONMIX also calculates the specific heat, $(\partial E / \partial T)_V$, and the temperature derivative of the average charge state, $(\partial \langle Z \rangle / \partial T)_V$, by numerical differentiation.

4. RADIATIVE PROPERTIES

4.1. Absorption, Emission, and Scattering Coefficients

The radiative properties of the plasma are calculated using a hydrogenic ion model for the cross sections. The absorption and emission coefficients include contributions from free-free (bremsstrahlung), bound-free (photoionization), and bound-bound (photoexcitation) transitions.

The general forms for the absorption coefficient and emissivity can be written respectively as [5]

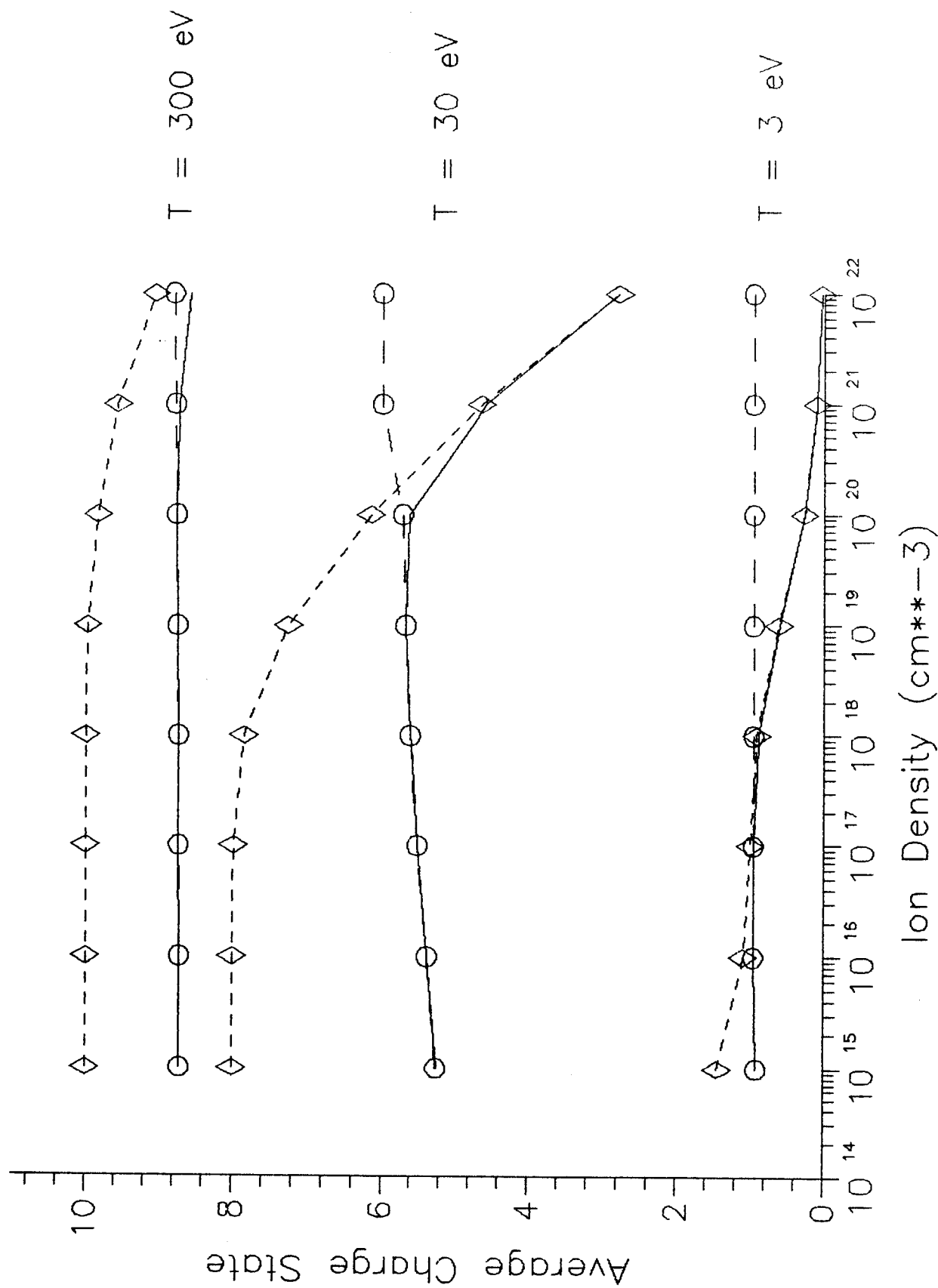


Figure 3-1. Average charge state for a neon plasma as a function of density at temperatures of 3, 30, and 300 eV. Results are shown from calculations assuming 2-body recombination only (dashed lines with circles), 3-body recombination only (dashed lines with diamonds), and both 2- and 3-body recombination (solid lines).

$$\begin{aligned}
\kappa_\nu = & \sum_k \sum_j \left\{ \sum_n \sum_{m>n} \left[n_{njk} - \left(\frac{g_{njk}}{g_{mjk}} \right) n_{mjk} \right] \alpha_{nm}^{bb}(\nu) \right. \\
& + \sum_{n>n'} \left[n_{njk} - n_{njk}^* e^{-h\nu/k_B T} \right] \alpha_n^{bf}(\nu) \\
& \left. + n_e n_{j+1,k} \alpha^{ff}(\nu) (1 - e^{-h\nu/k_B T}) \right\}
\end{aligned} \tag{4-1}$$

and

$$\begin{aligned}
\eta_\nu = & \left(\frac{2h\nu^3}{c^2} \right) \sum_k \sum_j \left\{ \sum_n \sum_m \left(\frac{g_{njk}}{g_{mjk}} \right) n_{mjk} \alpha_{nm}^{bb}(\nu) \right. \\
& \left. + \sum_{n>n'} n_{njk}^* e^{-h\nu/k_B T} \alpha_n^{bf}(\nu) + n_e n_{j+1,k} \alpha^{ff}(\nu) e^{-h\nu/k_B T} \right\}
\end{aligned} \tag{4.2}$$

where n' is determined by the photoionization cutoff energy $h\nu_{n'} = \phi_{jk} (n_0/n')^2$, and

$$n_{njk}^* = n_{0,j+1,k} n_e \cdot 1.66 \times 10^{-22} \left(\frac{g_{njk}}{g_{0,j+1,k}} \right) T^{-3/2} e^{(\phi_{jk} - \Delta E_{nn_0})/T}$$

is the LTE population of state n_{njk} using the computed ion density of the post-ionization ground state. The α 's represent the cross sections of the various transitions and are defined below. The indices j and k again refer to the ionization state and gas species, respectively. h , c , k_B , and ν as usual represent Planck's constant, the speed of light, Boltzmann's constant, and the photon frequency. All other symbols have been defined in previous sections.

The terms from left to right in equations (4-1) and (4-2) represent the contributions from bound-bound, bound-free, and free-free transitions. The second term inside each of the square brackets in eq. (4-1) is the

contribution from stimulated (induced) emission to the absorption coefficient. Note that in the high density limit (i.e., LTE), $n_m = n_n (g_m/g_n) e^{-\Delta E/T}$ and $n_n = n_n^*$. Thus, the correction for stimulated emission for all 3 transitions reduces to the LTE form, $(1 - \exp(-h\nu/k_B T))$, and the relation between the absorption coefficient and emissivity is given by the well-known Kirchhoff-Planck relation, $\eta_\nu = \kappa_\nu B_\nu$ (where B_ν is the Planck function). Because this relation will not be true in general, IONMIX tabulates the opacities for absorption and emission separately.

The cross section for free-free transitions in the hydrogenic approximation is [11]

$$\alpha_{ff}(\nu) = \frac{(2.40 \times 10^{-37} \text{ cm}^5) \cdot j^2 \overline{g_{ff}}}{(h\nu)^3 T^{1/2}} \quad (4-3)$$

where $h\nu$ is the photon energy in eV. For the free-free Gaunt factor, we use a simple fit to the results of Karzas and Latter [12]

$$\overline{g_{ff}} = 1 + 0.44 \exp\left\{-\frac{1}{4} \left(\gamma^2 + \frac{1}{4}\right)^2\right\}$$

where

$$\gamma^2 \equiv \log_{10}(13.6 \cdot \overline{Z_k^2}/T)$$

and

$$\overline{Z_k^2} \equiv \sum_{j=1}^{Z_k} j^2 f_{jk}$$

is the mean of the square of the ion charge state. The bound-free cross section is [5]

$$\alpha_n^{bf} = \frac{(1.99 \times 10^{-14} \text{cm}^2) \cdot F_u(j+1)^4}{n^5(h\nu)^3} \quad (4-4)$$

where F_u is the unoccupied fraction of the shell with principal quantum number n .

The bound-bound cross-section is a function of the oscillator strength, f_{nm} , and the line shape function $L(\Gamma, \nu)$ [5]:

$$\alpha_{nm}^{bb} = (2.65 \times 10^{-2} \text{cm}^2 \text{s}) \cdot f_{nm} L(\Gamma, \Delta\nu) . \quad (4-5)$$

IONMIX will compute the line shapes using either a Lorentzian profile or a Voigt profile (default). The expression for the Lorentzian profile is

$$L_L(\Gamma, \Delta\nu) = \frac{\Gamma/4\pi^2}{(\Delta\nu)^2 + (\Gamma/4\pi)^2}$$

where $\Delta\nu$ is the photon frequency shift from the line center, and Γ is the damping factor due to natural, Doppler (thermal), and collisional broadening:

$$\begin{aligned} \Gamma &= \Gamma_{\text{nat}} + \Gamma_{\text{Dop}} + \Gamma_{\text{coll}} \\ &= (2.29 \times 10^6)(\Delta E_{nm})^2 \\ &\quad + (1.41 \times 10^{11})\Delta E_{nm}\langle v \rangle + (4.58 \times 10^6)\langle v \rangle n_{\text{tot}}^{1/3} . \end{aligned}$$

$\langle v \rangle \equiv (T/A)^{1/2}$ is proportional to the mean thermal velocity, A is the atomic weight of the ion in amu, and ΔE_{nm} is the energy of the transition. The Voigt line profile is

$$L_V(\Gamma, \Delta\nu) = H(\Gamma, \Delta\nu, \Delta\nu_D) / (\pi^{1/2} \Delta\nu_D)$$

where $\Delta\nu_D$ is the Doppler shift, and $H(r, \Delta\nu/\Delta\nu_D)$ is the Voigt function, which depends on the frequency shift and the ratio of the Doppler damping factor to the sum of the natural plus collisional damping factors. The reader is referred to ref. [5] for a discussion of the Voigt function properties.

The scattering coefficient is used in calculating the radiative transport properties of the plasma. IONMIX considers contributions from Thomson electron scattering and plasma waves. We use the classical form of the Thomson cross section, which is reliable for low to moderate X-ray energies ($\lesssim 10^4$ eV) [5]:

$$s_v^T = (6.66 \times 10^{-25} \text{ cm}^2) n_e^\dagger \quad (4-6)$$

where n_e^\dagger is the effective electron density in cm^{-3} , which includes contributions from each bound electron for which the photon energy is greater than its binding energy. Thomson scattering becomes a dominant contributor to the Rosseland opacity at relatively high temperatures and low densities.

The scattering of photons by plasma oscillations can occur at low photon energies and high electron densities ($\gtrsim 10^{19} \text{ cm}^{-3}$). The plasma wave scattering coefficient can be written as [13]

$$s_v^P = \begin{cases} (\omega_p^2 - \omega^2)^{1/2}/c, & \text{if } h\nu \leq \hbar\omega_p \\ 0 & \text{if } h\nu > \hbar\omega_p \end{cases} \quad (4-7)$$

where

$$\omega_p = (4\pi e^2 n_e / m_e)^{1/2}$$

is the plasma frequency, e is the electron charge, and m_e is the electron mass.

The absorption and emission coefficients for a plasma of 90% Ar and 10% Li are plotted as a function of photon energy in Figures 4-1 and 4-2, respectively. The temperature in the calculation is 5 eV and the density is $3 \times 10^{17} \text{ cm}^{-3}$. The bound-bound transitions and photoionization edges are clearly visible in both figures. The peaks in the emission coefficients become smaller relative to absorption coefficients as the photon energy increases. This is because the populations move farther from LTE as the energy of the transition increases (see eq. (2-12)).

4.2. Opacity Calculations

The Rosseland and Planck mean opacities are obtained by integrating the absorption, emission, and scattering coefficients over the photon energy. The Rosseland mean opacities are generally used in determining the transport characteristics of radiation through a medium, while the Planck mean opacities are used to calculate the rates of energy exchange between the plasma and radiation. IONMIX computes Planck and Rosseland mean group opacities for up to 50 photon energy bins. Planck mean opacities for absorption and emission are computed separately because local thermodynamic equilibrium cannot be assumed.

The Planck mean group opacities for absorption and emission in the photon energy range from $x_g \equiv h\nu_g/kT$ to $x_{g+1} \equiv h\nu_{g+1}/kT$ are defined by [5]

$$\sigma_{p,g}^A = \frac{1}{\rho} \frac{\int_{x_g}^{x_{g+1}} dx B_\nu(T_R) \kappa_\nu}{\int_{x_g}^{x_{g+1}} dx B_\nu(T_R)} \quad (4-8)$$

and

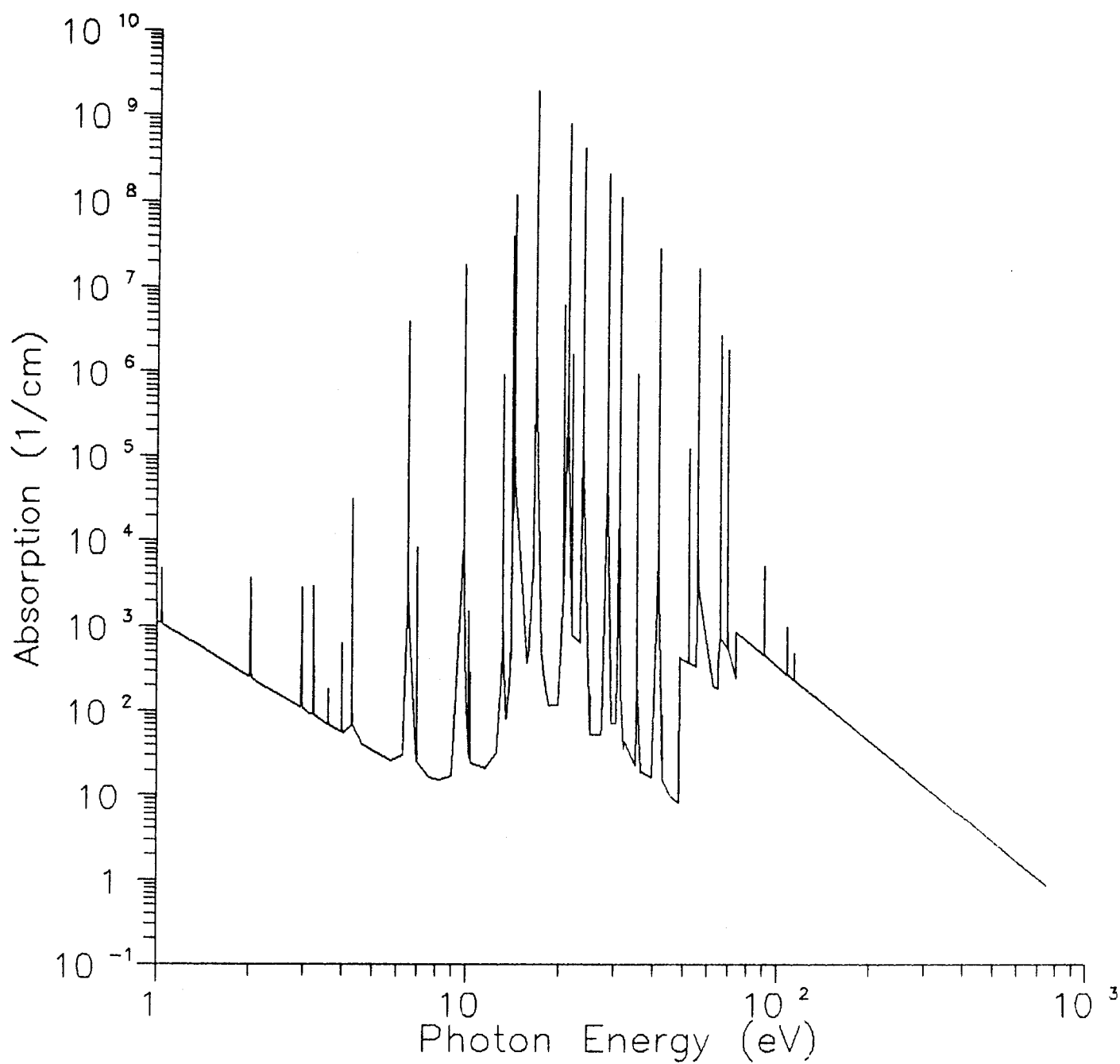


Figure 4-1. Absorption coefficient vs. photon energy for a plasma of 90% Ar and 10% Li. The temperature is 5 eV and density is $3 \times 10^{17} \text{ cm}^{-3}$.

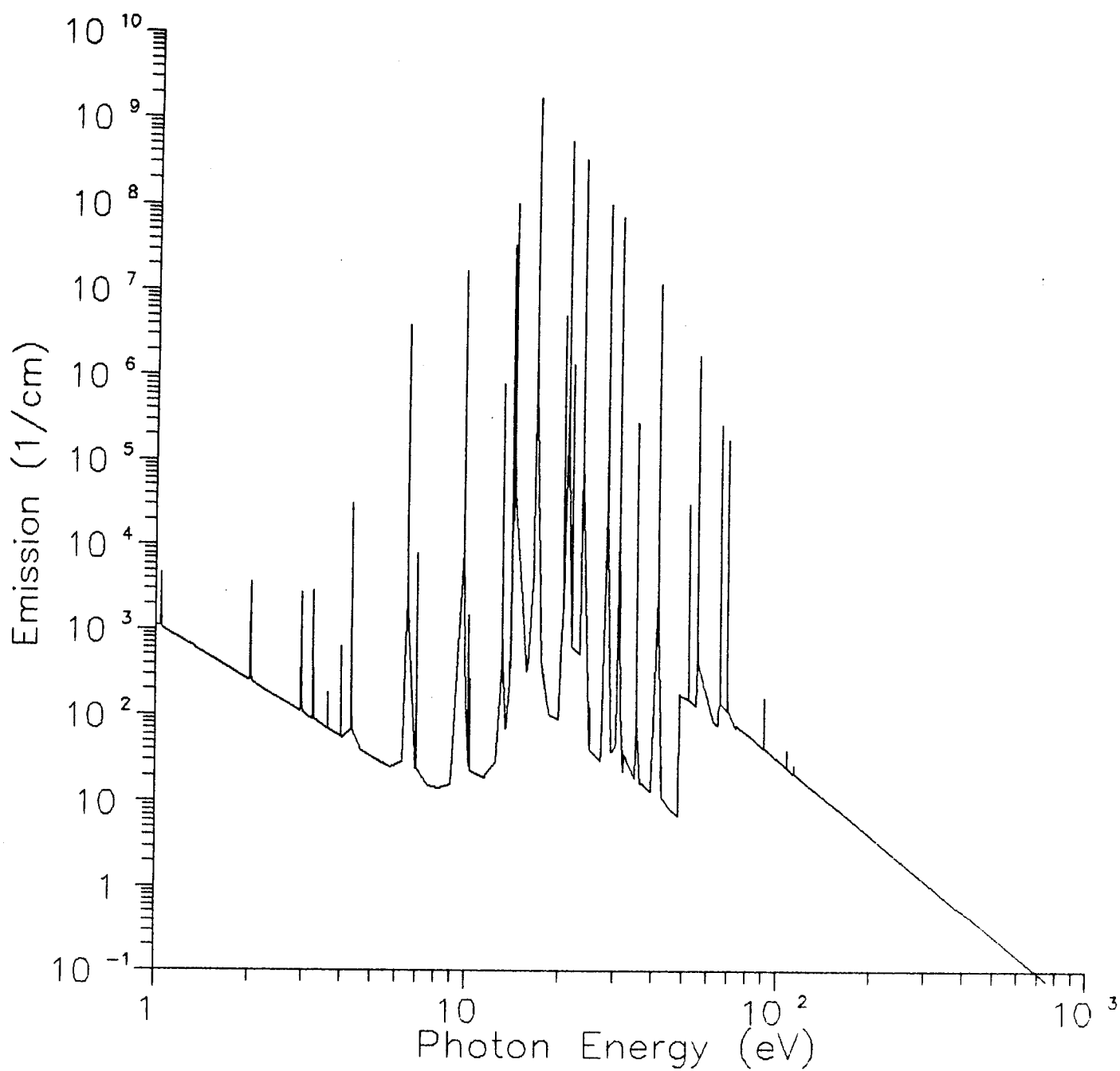


Figure 4-2. Emission coefficient vs. photon energy for a plasma of 90% Ar and 10% Li. The temperature is 5 eV and density is $3 \times 10^{17} \text{ cm}^{-3}$.

$$\sigma_{p,g}^E = \frac{1}{\rho} \frac{\int_{x_g}^{x_{g+1}} dx \eta_v}{\int_{x_g}^{x_{g+1}} dx B_v(T_R)} \quad (4-9)$$

where ρ is the mass density, and κ_v and η_v are defined in eqs. (4-1) and (4-2). $B_v(T_R)$ is the Planck function characterized by the radiation temperature T_R . The Rosseland mean group opacity is determined from a weighted average of the inverse of the total extinction coefficient, $\kappa_v + s_v$. In this case, the radiative coefficients are weighted by the temperature derivative of the Planck function:

$$\sigma_{R,g} = \frac{1}{\rho} \frac{\int_{x_g}^{x_{g+1}} dx \left(\frac{\partial B_v}{\partial T_R} \right)}{\int_{x_g}^{x_{g+1}} dx \left(\frac{\partial B_v}{\partial T_R} \right) \frac{1}{\kappa_v + s_v}} \quad (4-10)$$

As illustrated in Figure 4-1, the absorption and emission coefficients are not smoothly varying functions of the photon energy. Thus, to evaluate the opacity integrals with the desired accuracy, κ_v and η_v must be evaluated at a number of strategically placed points. Examples of this include points on either side of each photoionization edge, and several points in the vicinity of each bound-bound transition energy.

The integration scheme employed to evaluate the group opacities is a trapezoidal method using logarithmic interpolation between adjacent points. By placing a reasonable number of mesh points near each line transition energy (~ 5 to 10) and photoionization edge (2), the numerical accuracy of the integration is ~ a few per cent. Thus, the numerical inaccuracies are smaller than the uncertainties introduced by our relatively simple physical models.

The mean opacities integrated over all photon energies are computed by the group opacities:

$$\sigma_{P,tot} = \left[\sum_g \sigma_{P,g} \int_{x_g}^{x_{g+1}} dx B_\nu(T_R) \right] / \left[\int_0^\infty dx B_\nu(T_R) \right] \quad (4-11)$$

and

$$\sigma_{R,tot} = \left[\int_0^\infty dx \left(\frac{\partial B_\nu}{\partial T_R} \right) \right] / \left[\sum_g \sigma_{R,g}^{-1} \int_{x_g}^{x_{g+1}} dx \left(\frac{\partial B_\nu}{\partial T_R} \right) \right] . \quad (4-12)$$

The plasma emission rate, or "cooling rate", is then readily obtained from the Planck mean opacity for emission. For low density plasmas, the cooling rate (per ion per free electron) is only weakly dependent on the density. It is defined as

$$\Lambda(T) = \frac{4\sigma_{SB}\rho T^4}{n_e n_{tot}} \sigma_{P,tot}^E \quad (4-13)$$

where σ_{SB} is the Stefan-Boltzmann constant. Examples of computed cooling curves are shown in section 9.

5. FILE DESCRIPTIONS

The IONMIX code uses up to ten different logical units for input and output. The logical unit numbers are listed in Table 5-1 along with the corresponding file name, file type, and a brief description of its contents.

The only input file that must be supplied for all calculations is the one containing the namelist input, IONMXINP (see sec. 8 for a description of its contents, and Appendix A for a listing of a sample deck). Additional input files are required to supply ground state ionization potentials for elements

Table 5-1
Input/Output Files

Name*	Type	Unit number	Description
IONMXINP	Input	5	Namelist input file
IONMXOUT	Output	6	Text output file
ATOMnn	Input	7	File containing ionization potentials and electron shell occupation numbers for a gas of atomic number "n"
CNRDEOS	Output	8	Equation of state and opacity data file in a format required by CONRAD
IMPL0T01	Output	11	Plot file containing absorption coefficient data
IMPL0T02	Output	12	Plot file containing opacities as a function of temperature
IMPL0T03	Output	13	Plot file containing emission coefficient data
IMPL0T04	Output	14	Plot file containing opacities as a function of density
IMPL0T05	Output	15	Plot file containing charge states and cooling rates as a function of temperature
IMPL0T09	Output	19	Plot file containing fractional ionization populations as a function of temperature

* All file names have the usual ".DAT" VAX extension.

which do not have default values. IONMIX supplies default ionization potentials for the following elements: H, He, Li, Be, C, N, O, Ne, Mg, Si, S, Fe, Ar, Kr, and Xe. For other elements, the potentials are supplied through files called ATOMnn.DAT, where "nn" is the atomic number of the element.

Table 5-2 lists a sample file that could be used for oxygen. There is only 1 floating point number per record. The first record of the file should contain the data for the neutral atom, the second the data for the singly ionized particle, and so forth. Free format is used to read in the data. The data for each gas species must reside in its own file.

All results for the equations of state and opacities are written to the formatted file IONMXOUT.DAT. Additional output useful for plotting results is contained in the files IMPL0Tmm.DAT (mm=01-09; see sec. 8 for details). Finally, equation of state and opacity data tables can be written in a format that is used by radiation-hydrodynamics codes, such as MF-FIRE and ZPINCH [14].

6. SUBROUTINES AND THEIR FUNCTIONS

A flow diagram of the IONMIX subroutines is shown in Figure 6-1. All subroutines are written in FORTRAN 77 with the sole exception being the namelist read in the subroutine INPUT. Two VAX system subroutines are called: IDATE and TIME. Otherwise, the program is transportable to other mainframe computers.

Listed below is the name of each subroutine, and a brief description of its primary function.

Table 5-2

Sample input deck for ATOM08.DAT

16.4
38.2
60.7
82.8
122.
146.
699.
836.

IONMIX FLOW DIAGRAM

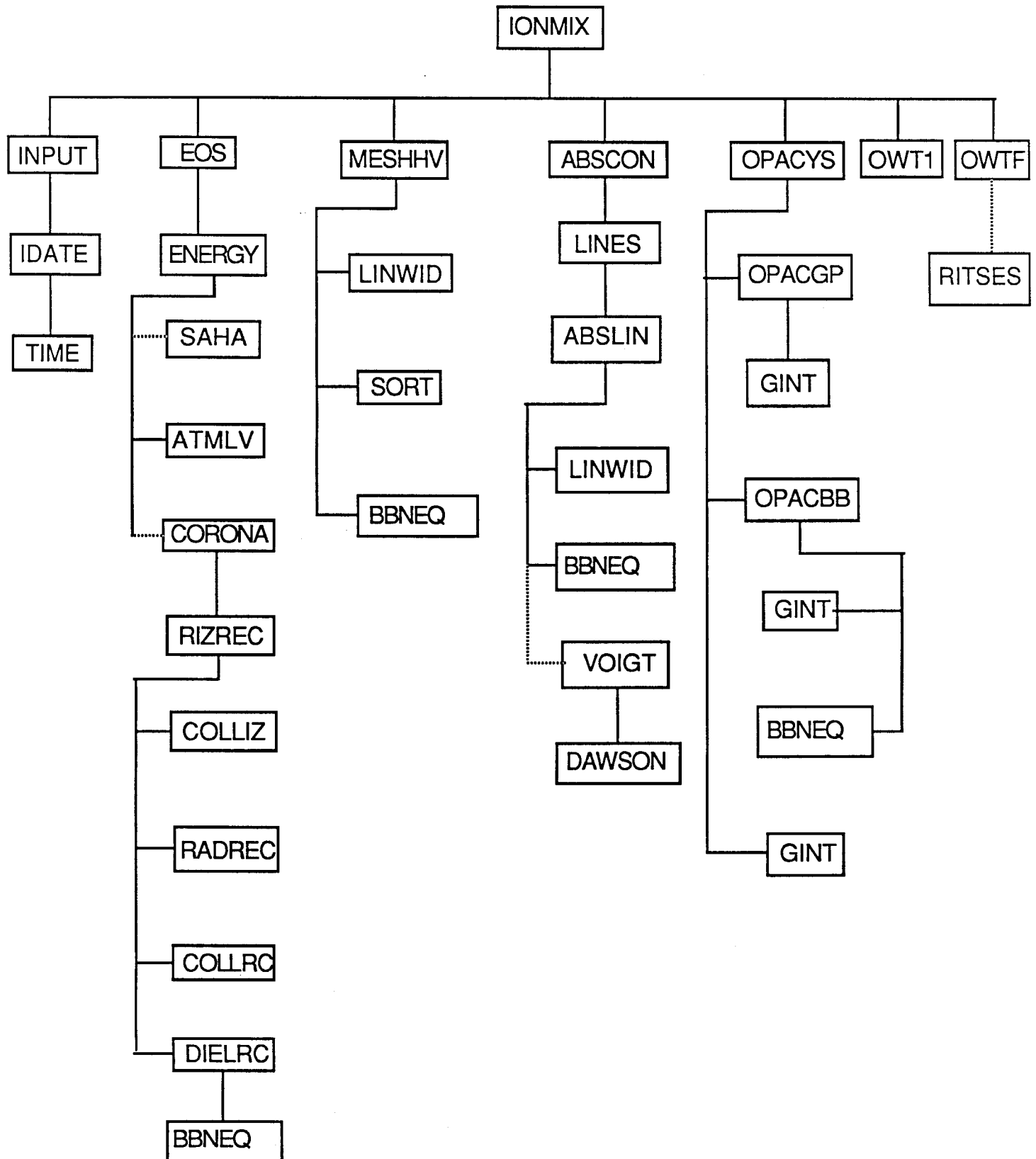


Figure 6-1. Flow diagram for the IONMIX code. Dotted lines indicate conditional routes.

<u>Name</u>	<u>Subroutine purpose</u>
ABSCON	Calculates the absorption, emission, and scattering coefficients for an array of photon energies.
ABSLIN	Computes the absorption for a specified bound-bound transition in which the principal quantum number changes.
ATMLV	Calculates the populations of atomic levels within a specified ionization state.
BBNEQ	Returns the effective energy, oscillator strength, and Gaunt factor for bound-bound transitions in which the principal quantum number does not change.
COLLIZ	Calculates the collisional ionization rate between two ionization states.
CORONA	Calculates the ionization populations according to the coronal model.
DAWSON	Returns the result of Dawson's integral.
DEBUG	Called by each subroutine to check if debug output is requested.
DIELRC	Computes the dielectronic recombination rate for a particular ionization state.
ENERGY	Finds the ionization and excitation populations for each gas species, and computes the specific energy.
EOS	Returns the specific energy and charge state, and their derivatives with respect to temperature.
GINT	Returns the integral of GINTn, where "n" = 1 through 6.
GINTn	Returns the integral of any of six ("n" = 1 through 6) different functions from zero to the specified value. These are generally some integral of a weighted Planck function.
IDATE	Returns date of calculation (VAX system subroutine).
INPUT	Sets default values, and reads input data from files.
IONMIX	Driver routine (main program).
LINES	Sums the contribution to the absorption coefficient from all bound-bound transitions.
LINWID	Computes the width of an absorption line due to natural, Doppler, and collisional broadening.
MENU	Block data routine which initializes constants and defines variables in common blocks.

MESHHV	Sets up the array of photon energies at which the absorption coefficients are to be evaluated.
OPACBB	Computes the contribution to the group opacity from all bound-bound transitions.
OPACGP	Calculates the Planck (absorption and emission) and Rosseland group opacities for a specified photon energy interval.
OPACYS	Finds the Planck (absorption and emission) and Rosseland opacities for each energy group, and calculates the mean values over all photon energies.
OWT1	Writes results for each temperature, density point as the calculation progresses.
OWTF	Writes final output information, including equation of state and opacity data tables.
RADREC	Computes the radiative recombination rate for a particular ionization state.
RITSES	Writes results to a file using a SESAME-like format.
RIZREC	Returns the ratio of the total ionization rate to total recombination rate.
SAHA	Computes the ionization populations according to the Saha model.
SORT	Arranges the photon energy array into ascending order.
TIME	Returns time of calculation (VAX system subroutine).
VOIGT	Calculates the Voigt profile for bound-bound transitions.

7. COMMON BLOCKS

Listed below are the common blocks used in IONMIX, the variables contained in each, and a brief description of each variable.

COMMON / CONSTS /

- 1) PI ratio of circular circumference to diameter (3.14159)
- 2) AVGDRO Avogadro's number (6.022×10^{23})
- 3) SBCON Stefan-Boltzmann constant (5.667×10^{-5} erg/cm²/s)
- 4) HPLANK Planck's constant (4.136×10^{-15} eV s)

COMMON / CONTRL /

- 1) ISW array of control switches
- 2) CON array of real constants

- 3) IPLOT array of control switches for plot data files
- 4) DTHEAT fractional temperature increment for computing derivatives of the specific energy and charge state
- 5) CRITSC critical value for switching between Saha and coronal ionization models

COMMON / DEBUGCM /

- 1) NOBUG logical flag; "true" if no debug output is requested
- 2) NCYCLD debug output is printed every "ncycld"th cycle
- 3) ICYCLD cycle counter for each subroutine name

COMMON / GASES /

- 1) NGASES number of gas species
- 2) IZGAS atomic number of each gas species
- 3) ATOMWT atomic weight of each gas species
- 4) AVGATW average atomic weight
- 5) AVGATN average atomic number
- 6) FRACSP number fraction of each gas species, relative to the total number of nuclei
- 7) FRACIZ number fraction of nuclei of each ionization state, relative to the number of nuclei of the particular gas species
- 8) FRACLV number fraction of ions in each atomic level, relative to the number of ions in the particular ionization state
- 9) POT ionization potentials for each ionization state and each gas species (eV)
- 10) NUMOCC electron shell occupation number for each ionization state and each gas species

COMMON / OPACS /

- 1) NPTSPG number of photon energy mesh points per opacity group for which absorption coefficients are to be computed
- 2) NGRUPS number of photon energy groups for opacity calculations
- 3) ENGRUP photon energy group boundaries (eV)

COMMON / PARAMS /

- 1) NPQMAX maximum principal quantum number used in computing absorption coefficients
- 2) NPMAXP maximum principal quantum number used in computing populations
- 3) NFRQBB number of photon energy points near a line center at which absorption coefficients will be computed
- 4) NPRING principal quantum number of the valence electrons in their ground state, as a function of the number of bound electrons
- 5) NEOPEN number of open holes available in the valence shell
- 6) BBNTON constants for bound-bound transitions in which the principal quantum number does not change
- 7) DEF POT default ionization potentials (eV)
- 8) NOCCDF default electron shell occupation numbers

COMMON / STRNGS /

- 1) NAMEDB array of subroutine names for which debug output is requested
- 2) HEADER header record for output files; contains time and date of calculation

COMMON / TDMESH /

- 1) NTEMP number of plasma temperature points for calculation
- 2) NDENS number of density points for calculation
- 3) NTRAD number of radiation temperature points for calculation
- 4) TPLSMA plasma temperatures (eV)
- 5) DENSNN number density of all nuclei (cm^{-3})
- 6) TRAD radiation temperatures (eV)
- 7) DLGTMP logarithmic increment in plasma temperature
- 8) DLGDEN logarithmic increment in number density
- 9) DLGTRD logarithmic increment in radiation temperature

8. INPUT VARIABLES

Only one input file is required to run IONMIX. This file, IONMXINP, reads namelist input and primarily serves 4 purposes: (1) define the composition of the plasma, (2) set up the temperature, density grid over which the physical properties of the plasma will be evaluated, (3) request plotting and debugging output, and (4) override default values of various parameters. The names and a brief description of the namelist input variables are listed in Table 8-1. Also shown are the default values, and whether the variable type is real (RV) or integer (IV). Tables 8-2, 8-3, and 8-4 show the default values for the photon energy boundaries for the group opacity calculations, the integer control switches, and floating point parameters. The IPLIT array can be used to request formatted output for plotting purposes. The only other input files IONMIX might read are the data files containing the ionization potentials for each gas (see section 5). These files are read if ISW(1)=1.

Table 8-1.

Input Variables

<u>Variable</u>	<u>Type</u>	<u>Default Value</u>	<u>Description</u>
NGASES	IV	1	number of gas species (maximum=10)
IZGAS	IV	0	atomic number of each gas (maximum=54)
ATOMWT	RV	0.	atomic weight of each gas (amu)
FRACSP	RV	0.	relative abundance, by number, of each gas species
NTEMP	IV	1	number of plasma temperatures (maximum=20)
NDENS	IV	1	number of densities (maximum=20)
NTRAD	IV	0	number of radiation temperatures (maximum=20)
TPLSMA	RV	0.	plasma temperatures (eV)
DENSNN	RV	0.	number density of nuclei (cm ⁻³)
TRAD	RV	0.	radiation temperatures (eV)
DLGTMP	RV	0.	logarithmic increment in plasma temperature
DLGDEN	RV	0.	logarithmic increment in number density
DLGTRD	RV	0.	logarithmic increment in radiation temperature
NPTSPG	IV	5	number of photon energy mesh points per opacity group
NGRUPS	IV	20	number of photon energy groups for opacity multigroup calculation (maximum=50)
NFRQBB	IV	5	number of photon energy mesh points near each line (bound-bound transition)
GRUPBD	RV	see Table 8-2	photon energy group boundaries for opacity multigroup calculation
ISW	IV	see Table 8-3	control switches
CON	RV	see Table 8-4	real constants
IPLLOT	IV	0	plot file control switches (0 => no output; 1 => formatted output) IPLLOT(1) - absorption coefficients IPLLOT(2) - temperature, mean opacities IPLLOT(3) - emission coefficients IPLLOT(4) - density, mean opacities IPLLOT(5) - temperature, cooling rate, ionization state
DTHEAT	RV	0.01	fractional temperature increment for specific heat and charge state derivative calculation
CRITSC	RV	10.	critical value for switching between Saha and coronal ionization models

Table 8-2.

Default Photon Energy Group Boundaries

<u>Group number</u>	<u>Lower boundary (eV)</u>	<u>Upper boundary (eV)</u>
1	0.10	0.30
2	0.30	1.00
3	1.00	1.58
4	1.58	2.51
5	2.51	3.97
6	3.97	6.29
7	6.29	10.0
8	10.0	15.8
9	15.8	25.1
10	25.1	39.7
11	39.7	62.9
12	62.9	100.
13	100.	178.
14	178.	316.
15	316.	562.
16	562.	1,000.
17	1,000.	3,160
18	3,160.	10,000.
19	10,000.	100,000.
20	100,000.	100,000.

Table 8-3.

Control Switches

<u>Switch number</u>	<u>Default value</u>	<u>Description</u>
1	0	user supplies ionization potentials (0=>no; 1=>yes)
2	0	compute opacities (0=>yes; 1=>no)
3	0	request debug output (0=>no; 1=>yes)
4	0	compute heat capacity and dZ/dT (0=>yes; 1=>no)
5	0	copy input file to output file (0=>yes; 1=>no)
6	3	use Saha/Coronal ionization model (0=>interpolation model; 1=>Saha; 2=>Coronal; 3=>2-body and 3-body processes fully considered)
7	0	not used
8	0	format for eos/opacity table (0=>none; 1=>old CONRAD; 2=>SESAME; 3=>new CONRAD)
9	0	not used
10	0	not used
11	0	not used
12	0	restrict ions to ground state (0=>no; 1=>yes)
13	0	specify opacity group boundaries (0=>use default values; 1=>user specifies; 2=>use values based on temperature)
14	0	use Voigt or Lorentzian line profile (0=>Voigt; 1=>Lorentzian)
15	2	number of electronic excitations considered in opacity calculations
16	0	include dielectronic recombination in calculation of ionization states (0=>yes; 1=>no)
17	0	include bremsstrahlung in opacity calculation (0=>yes; 1=>no)
18	0	include photoionization in opacity calculation (0=>yes; 1=>no)
19	0	include bound-bound transitions in opacity calculation (0=>yes; 1=>no; 2=>yes, but integrate core/wing contributions separately)
20	0	include scattering in opacity calculation (0=>yes; 1=>no)

Table 8-4.

Real Constants

<u>Constant number</u>	<u>Default value</u>	<u>Description</u>
1	0.	not used
2	10^{-10}	minimum species concentration before considering bound-bound and bound-free contributions to the opacity
3	10^{-10}	minimum concentration of an ionization state before considering bound-bound and bound-free contributions to the opacity
4	10^{-10}	minimum concentration of an excitation state before considering bound-bound and bound-free contributions to the opacity
5	10^{10}	maximum photon energy range from a line's center (in units of FWHM's) for computing its contribution to the opacity
6	10.	when isw(19)=2, this divides the line core from the wings (in units of FWHM's)

9. SAMPLE CALCULATIONS

9.1. Example 1

The first example illustrates results for a low density nitrogen plasma. The density is 10^{14} atoms/cm³, and the temperature ranges from 1 eV to 100 keV. Under these conditions, the plasma is not in local thermodynamic equilibrium (LTE) as 2-body atomic processes are the dominant recombination mechanisms. Results for the specific energy, average charge state, and plasma cooling rate (per ion per free electron) are plotted in Figures 9-1 through 9-3. These results are a very weak function of the density at ion densities $\leq 10^{16}$ cm⁻³.

The dashed curves in Figures 9-2 and 9-3 are the results obtained by Post et al. [3].

9.2. Example 2

The second example shows the results for a high density SiO₂ plasma that is assumed to be in LTE. Results for the Rosseland mean group opacities between 10 and 1000 eV are shown in Figure 9-4 for a temperature of 500 eV and mass density of 0.1 g/cm³. The input and output files for this calculation are listed in Appendix A.

The IONMIX results can be compared with those obtained by Argo et al. [15], which are represented by the dashed lines in Figure 9-4.

9.3. Example 3

In the final example, we present results for the cooling rates of a "solar composition" mixture of H, He, C, N, O, Ne, Mg, Si, S, and Fe. The relative number densities are: $f_H=0.94$, $f_{He}=0.06$, $f_C=3.4 \times 10^{-4}$, $f_N=0.8 \times 10^{-4}$, $f_O=5.6 \times 10^{-4}$, $f_{Ne}=0.7 \times 10^{-4}$, $f_{Mg}=0.29 \times 10^{-4}$, $f_{Si}=0.34 \times 10^{-4}$, $f_S=0.16 \times 10^{-4}$, and

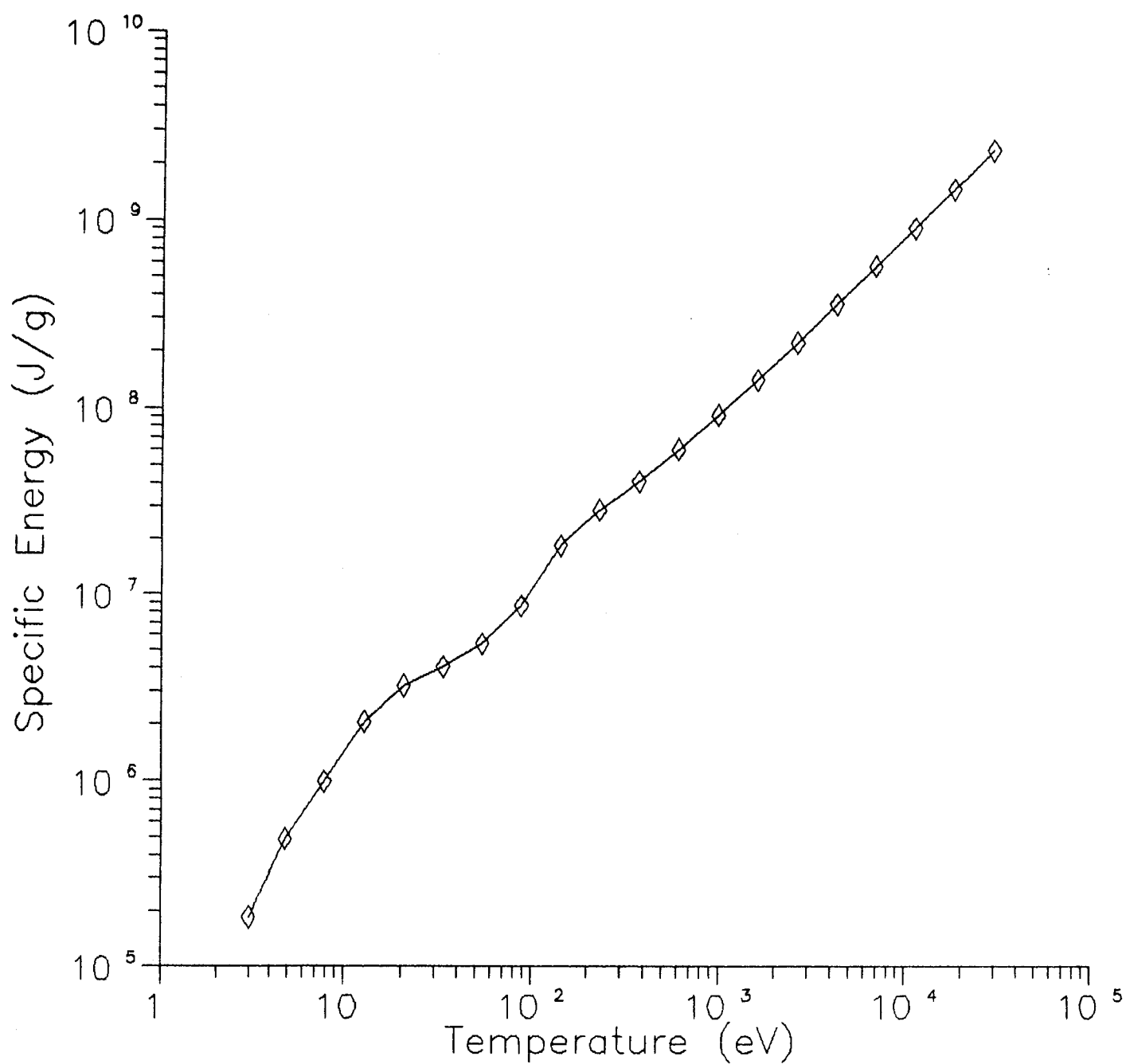


Figure 9-1. Specific energy vs. temperature for a low density nitrogen plasma.

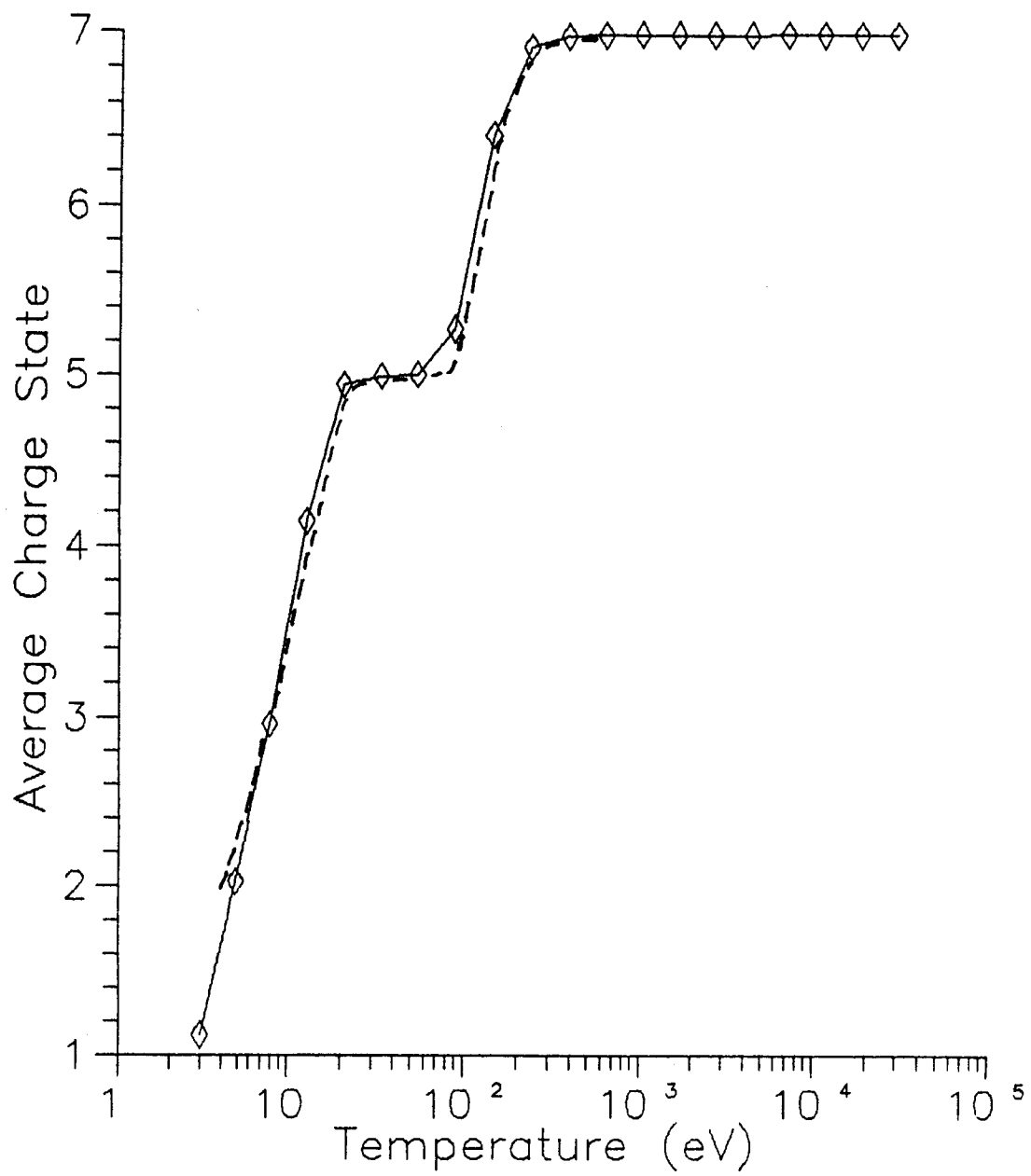


Figure 9-2. Average charge state vs. temperature for a low density nitrogen plasma.

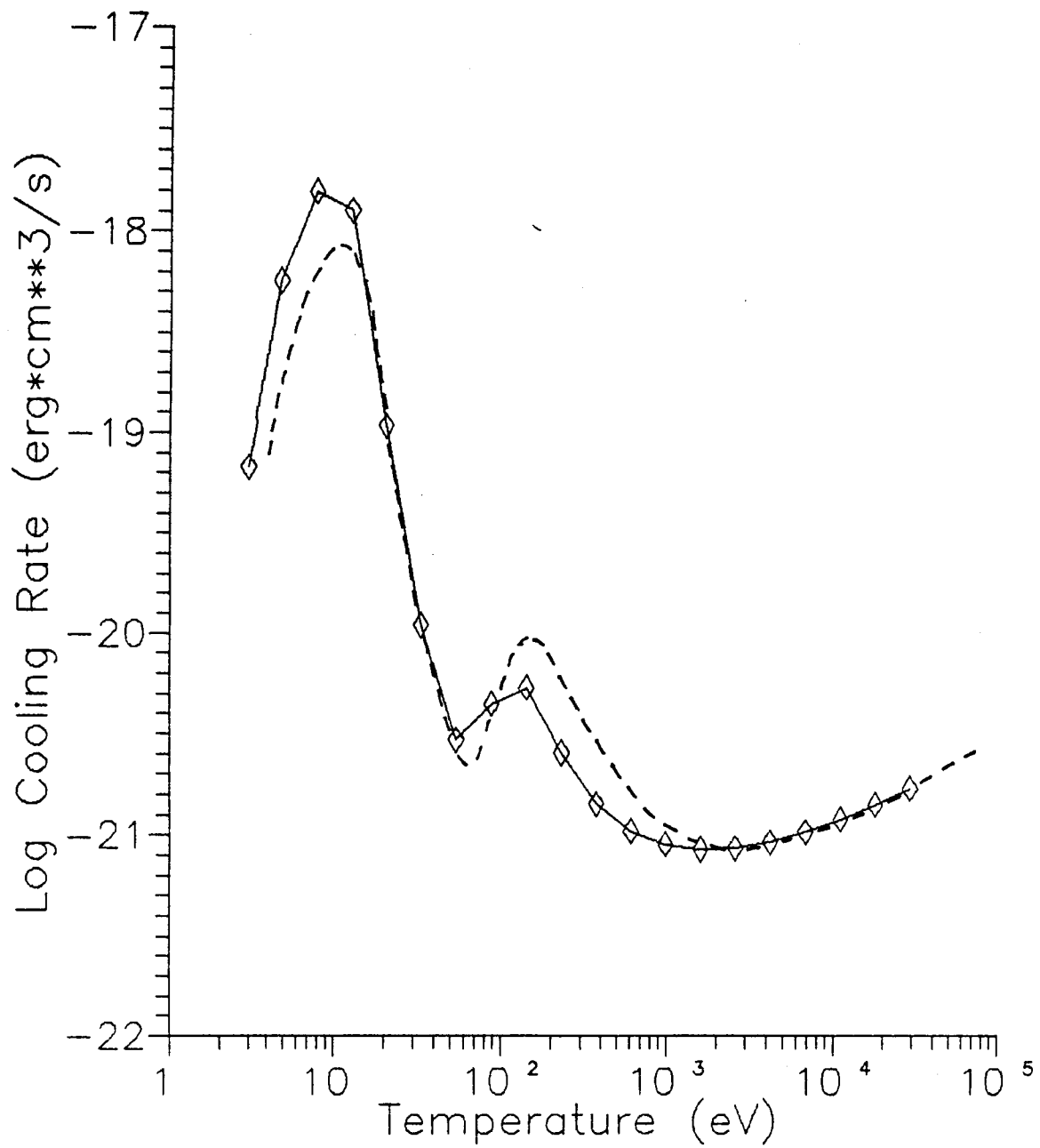


Figure 9-3. Plasma emission rate vs. temperature for a low density nitrogen plasma

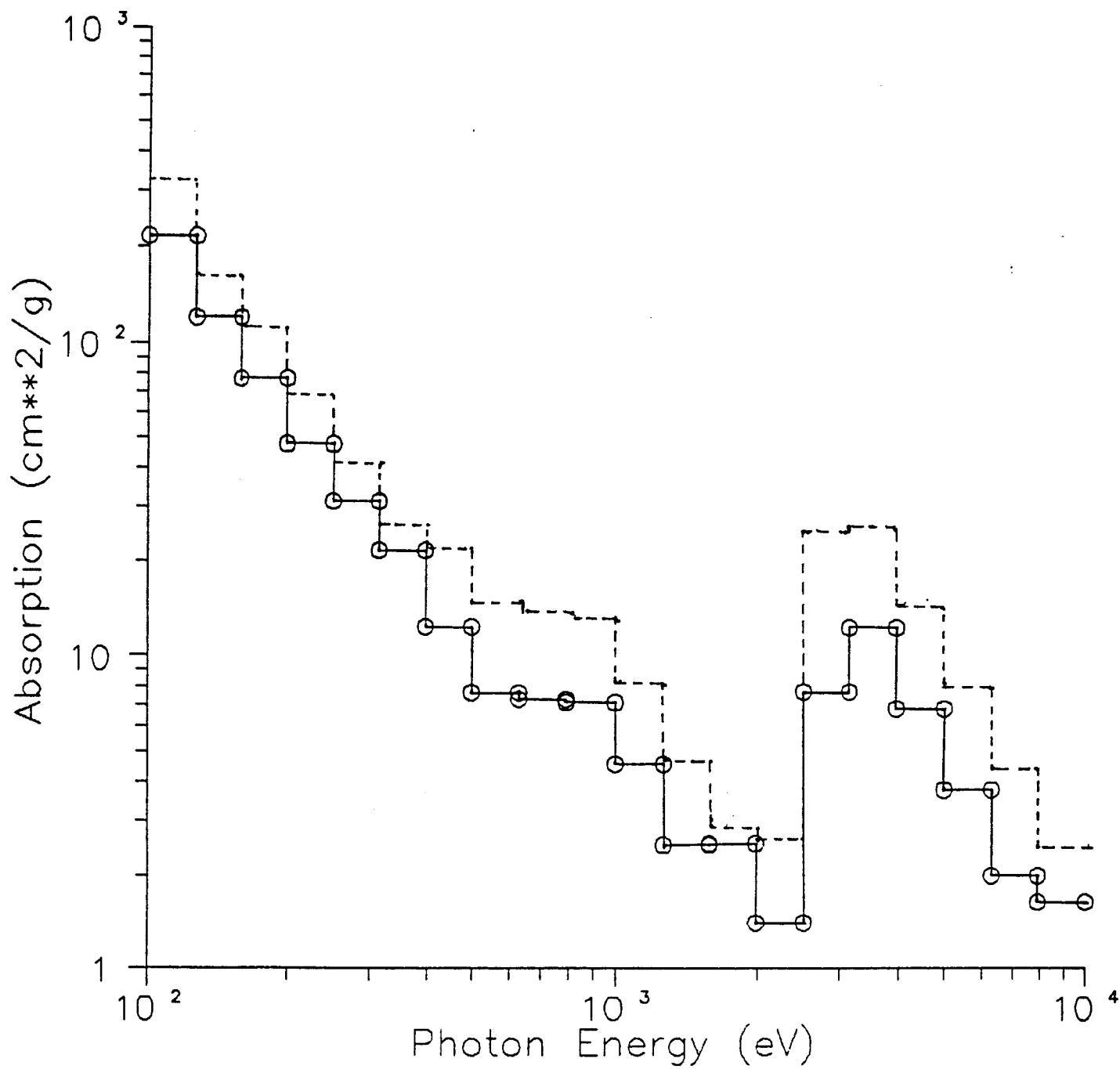


Figure 9-4. Rosseland group opacities vs. photon energy for a high density SiO_2 plasma. The temperature is 500 eV and density is 0.1 g/cm^3 .

$f_{Fe}=0.27 \times 10^{-4}$. The plasma emission rate is plotted in Figure 9-5 as a function of temperature. The ion density is 10^8 cm^{-3} . Although plasma is composed primarily of H and He, the greatest contribution to the emission rate at temperatures above $\sim 10^5 \text{ K}$ is due to the bound-bound transitions of the minor constituents.

The dashed line in Figure 9-5 is from the calculations of Shapiro and Moore [16].

ACKNOWLEDGEMENT

Support for this work has been provided by Lawrence Livermore National Laboratory. Computing support has been provided by the National Science Foundation through the San Diego Supercomputer Center.

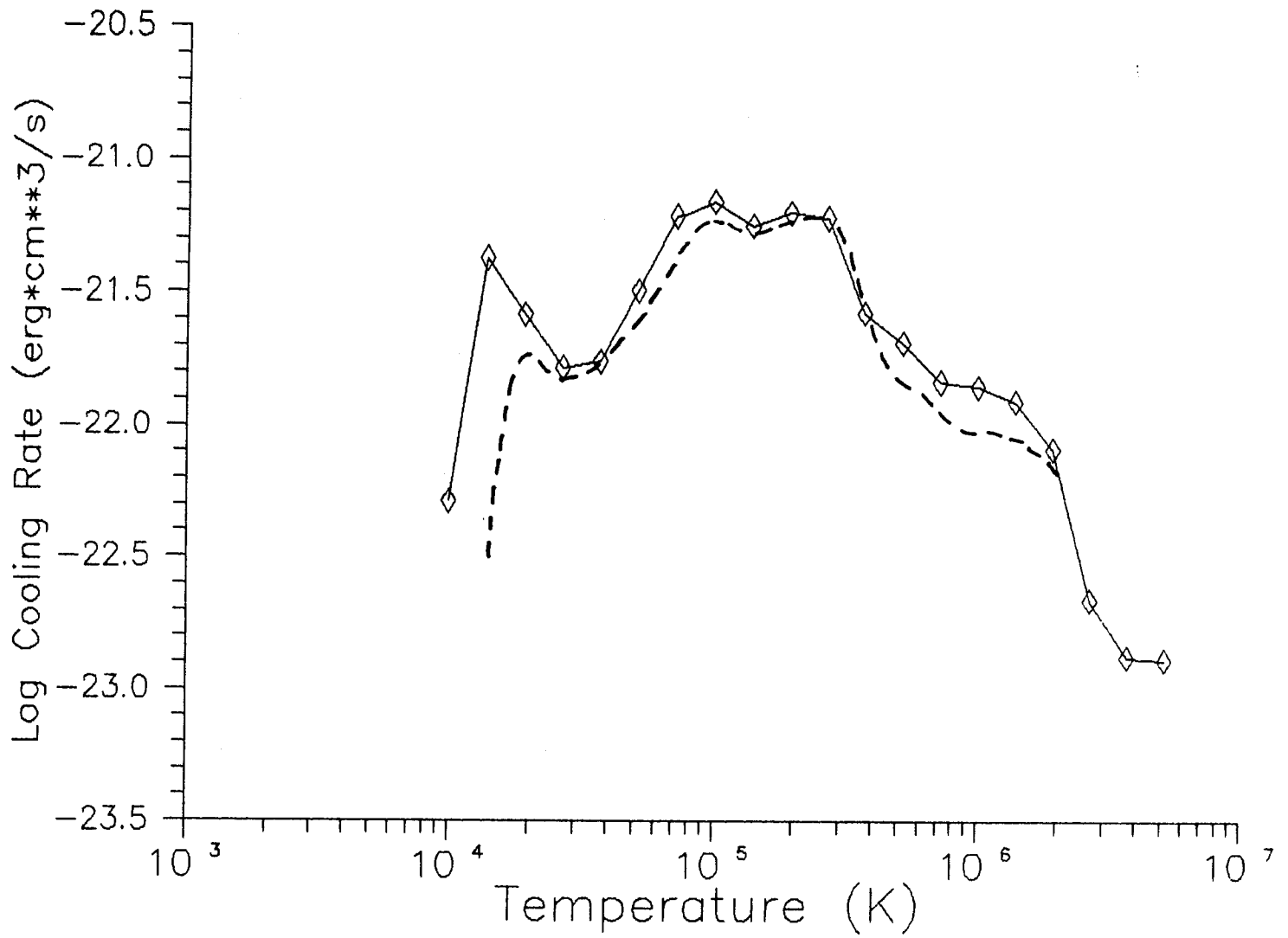


Figure 9-5. Plasma emission rate vs. temperature for a low density "solar composition" plasma.

REFERENCES

- [1] M. Uesaka, R.R. Peterson, and G.A. Moses, Nucl. Fusion 24 (1984) 1137.
- [2] See, e.g., "Radiation Hydrodynamics in Stars and Compact Objects," edited by D. Mihalas and K.-H.A. Winkler (Springer-Verlag, New York, 1986).
- [3] D.E. Post, R.V. Jensen, C.B. Tarter, W.H. Grasberger, and W.A. Lokke, At. Data Nucl. Data Tables 20 (1977) 397.
- [4] T.A. Carlson, C.W. Nestor, Jr., N. Wasserman, and J.D. McDowell, At. Data Nucl. Data Tables 2 (1970) 63.
- [5] D. Mihalas, "Stellar Atmospheres" (W. H. Freeman, San Francisco, 1978).
- [6] M.J. Seaton, Mon. Not. R. Astr. Soc. 119 (1959) 81.
- [7] M. Abramowitz and I.A. Stegun, "Handbook of Mathematical Functions" (Dover, New York, 1965).
- [8] A. Burgess, Astrophys. J. 141 (1965) 1588.
- [9] See, e.g., D.A. McQuarrie, "Statistical Mechanics" (Harper and Row, New York, 1976).
- [10] H. Van Regemorter, Astrophys. J. 136 (1962) 906.
- [11] Y.B. Zeldovich and Y.P. Raizer, "Physics of Shock Waves and High-Temperature Hydrodynamic Phenomena" (Academic Press, New York, 1966).
- [12] W.J. Karzas and R. Latter, Astrophys. J. Suppl. 6 (1961) 167.
- [13] R.R. Peterson and G.A. Moses, Comput. Phys. Commun. 28 (1983) 405.
- [14] G.A. Moses, R.R. Peterson, and T.J. McCarville, Comput. Phys. Commun. 36 (1985) 249; J.J. Watrous, G.A. Moses, and R.R. Peterson, University of Wisconsin Fusion Technology Institute Report UWFDM-584 (1985).
- [15] M.F. Argo and W.F. Huebner, J. Quant. Spectrosc. Radiat. Transfer 16 (1976) 1091.
- [16] P.R. Shapiro and R.T. Moore, Astrophys. J. 207 (1976) 460.

APPENDIX A

TEST RUN OUTPUT

Input File (see Section 9.2)

```
$data
  ngases = 2,
  izgas(1) = 14, 8,
  atomwt(1) = 28., 16.,
  fracsp(1) = 1., 2.,
  ntemp = 1,
  ndens = 1,
  tplsma(1) = 500.0,
  densnn(1) = 3.e21,
  ngrups = 20,
  nptspg = 2,
  nfrqbb = 10,
  iplot(1) = 1,
  isw(5) = 1,
  isw(6) = 1,
  isw(13) = 1,
  grupbd(1) = 100.,126.,158.,199.,251.,315.,397.,500.,629.,792.,1000.,
  grupbd(12)=1260.,1580.,1990.,2510.,3150.,3970.,5000.,6290.,7920.,1.e4,
$end
```

Output File

IONMIX calculation performed on Dec. 1, 1987 at 11:48:30

number of gases = 2

gas #	atomic #	number fraction	atomic weight
1	14	0.33333334	28.000
2	8	0.66666669	16.000

For gas # 1, with atomic # 14,
the ionization potentials are:

ionization state = 0	ionization potential = 7.260
ionization state = 1	ionization potential = 17.000
ionization state = 2	ionization potential = 34.300
ionization state = 3	ionization potential = 46.700
ionization state = 4	ionization potential = 159.800
ionization state = 5	ionization potential = 210.500
ionization state = 6	ionization potential = 261.300
ionization state = 7	ionization potential = 312.000
ionization state = 8	ionization potential = 364.000
ionization state = 9	ionization potential = 415.100
ionization state = 10	ionization potential = 503.700
ionization state = 11	ionization potential = 552.200
ionization state = 12	ionization potential = 2324.000
ionization state = 13	ionization potential = 2569.000

For gas # 2, with atomic # 8,
the ionization potentials are:

ionization state = 0	ionization potential = 16.400
ionization state = 1	ionization potential = 38.200
ionization state = 2	ionization potential = 60.700
ionization state = 3	ionization potential = 82.800
ionization state = 4	ionization potential = 121.900
ionization state = 5	ionization potential = 145.800
ionization state = 6	ionization potential = 698.800
ionization state = 7	ionization potential = 836.000

Switches used for current calculation

```

isw( 1) = 0 User supplies ionization potentials (0=>no)
isw( 2) = 0 Compute opacities ? (0=>yes)
isw( 3) = 0 Request debug output (# => # of subrts)
isw( 4) = 0 Compute heat cap. and dZ/dT ? (0=>yes)
isw( 5) = 1 Copy input file to output file (0=>yes)
isw( 6) = 1 Saha/Coronal model (0=>S/C, 1=>S, 2=>C, 3=>C w/ 3-body rec.)
isw( 7) = 0
isw( 8) = 0 Calculation to make a file for CONRAD ?
              (0=>no; 1,12=>CONRAD; 2,12=>SESAME)
isw( 9) = 0
isw(10) = 0
isw(11) = 0
isw(12) = 0 Restrict ions to ground state ? (0=>no)
isw(13) = 1 Specify group boundaries (0=>default)
              (1=>user specifies) (2=>default T-dep. values)
isw(14) = 0 Voigt or Lorentzian line profile (0=>V)
isw(15) = 2 Maximum prin. quantum # (0=>code picks)
              (if<0,npqmax=-isw15; if>0,npqmax=isw15+grnd.st.#)
isw(16) = 0 Include dielectronic recomb. ? (0=>yes)
isw(17) = 0 Include bremsstrahlung ? (0=>yes)
isw(18) = 0 Include photoionization ? (0=>yes)
isw(19) = 0 Include line contributions ? (0=>yes)
              (1=>no) (2=>core/wings computed separately)
isw(20) = 0 Include scattering contribs. ? (0=>yes)

```

Constants used for current calculation

```

con( 1) = 0.00E+00
con( 2) = 1.00E-10 min. species concentration to compute bb and bf transitions
con( 3) = 1.00E-10 min. ionization concentration to compute bb and bf transitions
con( 4) = 1.00E-10 min. concentration of an atomic state to consider bb and bf transitions
con( 5) = 1.00E+10 range, in # of line widths (fwhm), to compute contribution from a bb transition
con( 6) = 1.00E+01 width, in # of line widths (fwhm), of line core
con( 7) = 0.00E+00
con( 8) = 0.00E+00
con( 9) = 0.00E+00
con(10) = 0.00E+00

```

Plot files opened for current calculation

```

iplot( 1) = 1 Absorption coeffs. vs. photon energy
iplot( 2) = 0 Mean opacities vs. temperature
iplot( 3) = 0 Emission coeffs. vs. photon energy
iplot( 4) = 0 Mean opacities vs. density
iplot( 5) = 0 Charge and cool. rate vs. temp.
iplot( 6) = 0
iplot( 7) = 0
iplot( 8) = 0
iplot( 9) = 0 Ioniz. pop.s vs. temperature
iplot(10) = 0

```

 Results for next temperature, density point

Temperature = 5.000E+02 eV
 Number density = 3.000E+21 cm**3
 Mass density = 9.963E-02 grams/cm**3
 Electron density = 2.849E+22 cm**3
 Average charge state = 9.497E+00
 Specific energy = 5.642E+07 J/gram
 Pressure = 2.523E+13 dyne/cm**3
 Heat capacity = 8.528E+04 J/gram/eV
 d(Charge st.)/d(Temp.) = 1.099E-03 ev**1
 Max. prin. quantum # used to compute populations = 14
 Max. prin. quantum # used to compute absorp. coeffs. = 5 4
 Planck mean opacity (abs.) = 2.716E+01 cm**2/gram
 Planck mean opacity (ems.) = 2.716E+01 cm**2/gram
 Rosseland mean opacity = 3.190E+00 cm**2/gram
 Plasma cooling rate = -2.009E+01 erg*cm**3/sec (Log10 value)

Group opacities:

group number	lower boundary (eV)	upper boundary (eV)	Planck (abs) opacity (cm**2/g)	Planck (ems) opacity (cm**2/g)	Rosseland opacity (cm**2/g)
1	1.000E+02	1.260E+02	3.040E+02	3.039E+02	2.164E+02
2	1.260E+02	1.580E+02	1.326E+02	1.324E+02	1.199E+02
3	1.580E+02	1.990E+02	9.366E+01	9.344E+01	7.664E+01
4	1.990E+02	2.510E+02	4.792E+01	4.782E+01	4.739E+01
5	2.510E+02	3.150E+02	3.132E+01	3.126E+01	3.112E+01
6	3.150E+02	3.970E+02	5.313E+01	5.310E+01	2.159E+01
7	3.970E+02	5.000E+02	1.777E+01	1.776E+01	1.227E+01
8	5.000E+02	6.290E+02	2.731E+01	2.731E+01	7.617E+00
9	6.290E+02	7.920E+02	1.131E+01	1.131E+01	7.257E+00
10	7.920E+02	1.000E+03	7.202E+00	7.201E+00	7.073E+00
11	1.000E+03	1.260E+03	4.466E+00	4.466E+00	4.526E+00
12	1.260E+03	1.580E+03	2.425E+00	2.424E+00	2.484E+00
13	1.580E+03	1.990E+03	9.482E+01	9.482E+01	2.507E+00
14	1.990E+03	2.510E+03	2.283E+01	2.283E+01	1.405E+00
15	2.510E+03	3.150E+03	2.133E+01	2.133E+01	7.689E+00
16	3.150E+03	3.970E+03	1.283E+01	1.283E+01	1.225E+01
17	3.970E+03	5.000E+03	6.058E+00	6.058E+00	6.786E+00
18	5.000E+03	6.290E+03	2.949E+00	2.949E+00	3.745E+00
19	6.290E+03	7.920E+03	1.744E+00	1.744E+00	1.981E+00
20	7.920E+03	1.000E+04	4.456E-01	4.457E-01	1.630E+00